Low-Lying Excited States of C120 and C151: A Multireference Perturbation Theory Study

Tetsuya Sakata,[†] Yukio Kawashima,*[,†,‡] and Haruyuki Nakano[†]

Department of Chemistry, Graduate School of Sciences, Kyushu University, Fukuoka 812-8581, Japan, and Institute of Advanced Research, Kyushu University, Fukuoka 812-8581, Japan

Received: March 5, 2010; Revised Manuscript Received: October 6, 2010

Excited states of two 7-aminocoumarin derivatives, coumarin 120 (7-amino-4-methylcoumarin) and coumarin 151 (7-amino-4-trifluoromethylcoumarin), were investigated using generalized multiconfigurational quasidegenerate perturbation theory (GMC-QDPT), multiconfigurational quasidegenerate perturbation theory (MC-QDPT) and time-dependent density functional theory (TDDFT) with the B3LYP and CAM-B3LYP functionals. The absorption and fluorescence spectra of C120 and C151 were calculated. We elucidated the characters of the low-lying states of C120 and C151. The absorption spectra calculated with GMC-QDPT and TDDFT B3LYP agreed well with the experimental data, while for the fluorescence spectra, the TDDFT calculations overestimated the fluorescence spectra compared to GMC-QDPT calculations. Utilizing active spaces with large numbers of electrons and orbitals for reference functions, GMC-QDPT showed a better performance than MC-QDPT with a complete active space self-consistent field (CASSCF) reference of active space with smaller number of electrons and orbitals. In our gas phase calculation, we found that the optimized structures for the first excited states have a planar amino group with a CN single bond, while the amino group is pyramidal in the ground state.

Introduction

Multireference perturbation theory based on multiconfigurational reference functions has become a practical tool for studying the electronic structures of low-lying excited states. Multireference Møller−Plesset (MP) perturbation theory[1−3] and multiconfigurational quasidegenerate perturbation theory (MC-QDPT)[4,5] succeeded in describing the excited states of π conjugated systems by taking into account both static and dynamic electron correlations.[6−13] These methods include valence π and π^* orbitals in the active space of the reference complete active space self-consistent field (CASSCF) wave function to perform calculations of the $\pi \rightarrow \pi^*$ excited states. However, the use of a CASSCF wave function limits the application of these methods to large π conjugated systems because the active space dimension grows rapidly with the number of active orbitals and electrons. To avoid this drawback, a perturbation theory using general multiconfiguration (GMC) SCF wave functions as reference functions (GMC-QDPT) was developed.[14−16] This method enables us to perform calculations of active space with large numbers of electrons and orbitals, which leads to wider application.

In this article, we apply GMC-QDPT to two 7-aminocoumarins, C120 (7-amino-4-methyl-1,2-benzopyrone) and C151 (7-amino-4-trifluoromethyl-1,2-benzopyrone), to study the excited states of these molecules and understand the absorption and fluorescence spectra with quantitative calculations. Figure 1 illustrates the skeletal formula of C120 and C151. 7-Aminocoumarins, or 4-methyl-7-diethylaminocoumarins, are the most studied dyes in the coumarin family. Substitution at the 7-position with an electron-donating group enhances the fluorescence of the dye, which leads to their wide application in blue-green laser dyes and fluorescence probes. Furthermore,

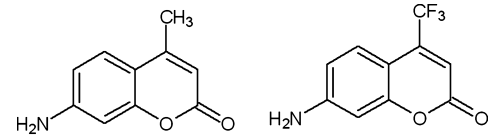

Coumarin 120 (C120) Coumarin 151 (C151)

Figure 1. Chemical structures of Coumarin 120 and Coumarin 151.

7-aminocoumarin dyes are applied to study solvatochromic properties because the large Stokes' shifts of these molecules are very sensitive to the polarity and viscosity of the surrounding solvent environment. Therefore, the photophysics of these dyes has been studied intensively.[17−39]

Among the 7-aminocoumarins, C120 and C151 are the most basic and well-studied compounds. For coumarin 120 (C120)[17] and coumarin 151 (C151),[18] it is known that the nonradiative deactivation process differs in polar and nonpolar solvents. Much effort has been expended to understand this process; however, the process, especially in nonpolar solvents, is not well understood. Two different mechanisms for the nonradiative deactivation process for 7-aminocoumarins have been proposed. The first mechanism describes the nonradiative deactivation process as the 7-aminocoumarin forming the so-called twisted intramolecular charge-transfer state from the S_1 singlet excited state.[19] The second is the so-called open-closed umbrella-like motion mechanism.[20] This mechanism ascribes the internal conversion process to a structural change of the amino group from a planar N^+-aromatic configuration (with sp^2 hybridization for the nitrogen atom) to a pyramidal N-aromatic configuration (with sp^3 hybridization for the nitrogen atom). More research on the excited states of 7-aminocoumarins is necessary to elucidate the nonradiative deactivation process.

The reasonable system size of C120 and C151 compared with the sizes of other 7-aminocoumarins allowed various quantum mechanical methods to be employed to study and understand

* Corresponding author. E-mail: snow@ccl.scc.kyushu-u.ac.jp.
† Graduate School of Sciences.
‡ Institute of Advanced Research.

10.1021/jp1019872
Published on Web 11/04/2010

the low-lying excited states. Semiempirical excited state calculations of 7-aminocoumarins in the gas phase have been reported by McCarthy and Blanchard.[21] Ando combined ab initio electronic structure calculations and molecular dynamics simulation to study the solvation dynamics of C120 in methanol.[22] A Carr−Parrinello molecular dynamics (CPMD) simulation was carried out to study microsolvated C151[23−25] utilizing the quantum mechanics (QM)/molecular mechanics (MM) CPMD method. Nguyen et al.[26] applied various density functionals and basis sets to C120 and C151 and assessed their performance. Cave et al.[27] performed TDDFT, CASSCF, and multistate CASPT2 calculations on coumarins C120 and C151. Recently, Kina et al. performed ab initio molecular dynamics of C151 in water at the CASSCF level with the use of an effective fragment potential.[28] In our previous work,[29] we elucidated the differences in the absorption spectra among some 7-aminocoumarins using TDDFT with the B3LYP functional. Despite continuing efforts, quantitative calculations have been limited to the absorption spectra, the fluorescence spectra not being calculated. Studies of fluorescence spectra are essential to understand the deactivation process of C120 and C151.

In this article, we aim to elucidate the characters of the low-lying excited states by calculating the absorption and fluorescence spectra of C120 and C151. This article is organized as follows. The computational details are described in the next section. The results of the calculations are shown and discussed in the third section. The article is concluded in the final section.

Computational Details

The calculations were carried out for the ground and low-lying singlet excited states of coumarin 120 and 151. The ground state geometries of the 7-aminocoumarins studied were optimized at the MP2 level, and the first excited state geometries were optimized using CIS and TDDFT.[40−45] We used B3LYP[46−48] and CAM-B3LYP[49] functionals for the TDDFT optimization. The excitation energy calculations were carried out by applying GMC-QDPT. We used multireference singles and doubles-type functions with 45 parent configurations to span the reference generalized configuration space (GCS) averaged over eight low-lying states. For comparison, the calculated absorption spectra were calculated also by MC-QDPT[4,5] and TDDFT with the B3LYP functional. For the MC-QDPT calculation, we employed CASSCF reference functions with various active spaces averaged over eight low-lying states. The fluorescence spectra calculated by GMC-QDPT are compared with the TDDFT calculations. For the CIS and B3LYP optimized structures, TDDFT B3LYP calculations were carried out, and for the CAM-B3LYP optimized structures, TDDFT CAM-B3LYP calculations were carried out. Dunning's cc-pVDZ basis set[50] was used for our calculation. The geometry optimization calculations were performed with the GAUSSIAN09 suite of programs[51] and GMC-QDPT and MC-QDPT calculations were carried out using the GAMESS program package.[52]

Results and Discussion

A. Ground State and Excited State Structures of C120 and C151. The optimized structures of the coumarin moiety in the ground state and the first excited state of C120 and C151 with the dipole moments of each structures are listed in Table 1. The molecular structure designation is illustrated in Figure 2. The bonds are designated by letters (a−n) and the bond angles are designated by numbers (1−15).

As seen in Table 1, the structures of C120 and C151 are very similar. We compared our MP2 optimized structures with the structure optimized at B3LYP level, listed in Figure S1 in the Supporting Information. The two structures agreed well and the difference has a very small influence to the absorption spectra. We therefore focus on a comparison between the ground state structure optimized at the MP2 level and the first excited state structure optimized at the CIS and TDDFT level.

Bonds a−f belong to the aromatic ring. In the ground state, the lengths of the bonds are between single and double C−C bonds, ranging from 1.385 to 1.409 Å for C120. On the other hand, bonds g−j show large bond length alternations in the ground state structure compared with those for the aromatic ring. The bond lengths of bonds g−j are between 1.358 and 1.456 Å.

In the excited state, bonds a−f in the aromatic rings show bond alternation, unlike the structure in the ground state. The bond length of a−f ranges from 1.390 to 1.442 in TDDFT B3LYP optimization, from 1.379 to 1.456 in TDDFT CAM-B3LYP optimization, and from 1.360 to 1.453 in CIS optimization. The CIS optimized structure and TDDFT CAM-B3LYP optimized structure show a similar tendency in the aromatic ring moiety. TDDFT B3LYP optimized structures have bond lengths between the MP2 ground state structures and CIS and TDDFT CAM-B3LYP structures. For bonds g−j for the other ring in the excited states, the bond alternation is small compared with that of the ground state structure. For bond g, TDDFT B3LYP structures show long bond distances, and for bond j, CIS shows a short bond distance. Otherwise, the optimized geometries of CIS, B3LYP and CAM-B3LYP show similar tendencies.

The sum of the bond angles (7−9) around the nitrogen atom in the ground state is 338.8° in C120 and 340.6° in C150. The amino group in the ground state has a pyramidal structure. In the excited state, the CIS optimized structure's amino group is slightly more planar than in the ground state and TDDFT optimized structures have a planar amino group. For bond m, the structures in the excited state have shorter bond lengths than the ground state structure. However, the bond length in the excited state is not as short as the bond length of the CN^+ double bond. Thus, the loose CN bond allows the flip-flop motion of the amino group. The Mulliken population charge of nitrogen atom of the amino group is −0.091 at S_0 state and −0.069 at S_1 state. The negative charge seen at the S_0 state reduces, but it does not become positive. The excited state structure becomes planar, but the nitrogen atom in the amino group is not cationic as described in ref 20.

The differences between CIS, B3LYP, and CAM-B3LYP were small, and the differences in these structures have a very small influence on the fluorescence spectra.

Kina et al. found two local minima in the excited state of C151. One minima corresponds to the local-excitation state, and the other minima corresponds to the charge-transfer (CT) state.[28] The former agrees with the optimized structure found in this article. We applied CAM-B3LYP in this study because this method is known to be applicable to CT states.[53] However, we were not able to find this structure in this study.

The calculated dipole moments for each optimized structures are listed in Table 1. For both C120 and C151, the dipole moments of the excited state are slightly larger than that of the ground state. The dipole moments of C120 are larger than that of C151.

B. Absorption Spectra. We utilized the GMC-QDPT method for calculating the vertical excitation energies from the ground state to study the absorption spectra. The use of GMCSCF wave functions as a reference for the perturbation calculations enables

TABLE 1: Optimized Geometry of the Ground State (GS) and First Excited State of C120 and C151

	C120				C151			
		first excited state				first excited state		
	GS MP2	B3LYP	CAM-B3LYP	CIS	GS MP2	B3LYP	CAM-B3LYP	CIS
				Bond Lengths (Å)				
A	1.408	1.422	1.428	1.434	1.411	1.419	1.422	1.434
B	1.385	1.393	1.379	1.366	1.383	1.388	1.373	1.360
C	1.409	1.421	1.423	1.420	1.411	1.415	1.427	1.427
D	1.396	1.415	1.407	1.407	1.396	1.421	1.404	1.402
E	1.393	1.390	1.380	1.369	1.391	1.405	1.381	1.371
F	1.405	1.442	1.456	1.458	1.406	1.409	1.444	1.453
G	1.449	1.454	1.417	1.400	1.443	1.489	1.435	1.404
H	1.358	1.404	1.412	1.410	1.357	1.391	1.404	1.408
I	1.456	1.426	1.418	1.427	1.459	1.430	1.422	1.427
J	1.395	1.457	1.442	1.395	1.391	1.454	1.435	1.395
K	1.374	1.347	1.338	1.335	1.375	1.348	1.343	1.335
L	1.217	1.218	1.211	1.189	1.216	1.215	1.209	1.188
M	1.398	1.370	1.367	1.369	1.393	1.365	1.356	1.358
N	1.501	1.493	1.494	1.503	1.503	1.470	1.479	1.496
				Bond Angles (deg)				
1	117.1	117.2	116.5	116.1	117.4	117.9	117.0	116.3
2	121.3	122.0	121.5	121.6	120.8	122.7	121.6	121.6
3	120.6	119.7	120.8	121.1	121.0	119.0	120.5	121.0
4	118.9	119.5	119.2	119.0	118.9	119.4	119.1	118.9
5	119.7	120.6	120.5	120.8	119.6	120.5	120.6	120.8
6	122.3	121.0	121.4	121.4	122.3	120.4	121.2	121.4
7	114.1	120.4	119.2	116.7	114.7	121.1	121.0	118.4
8	114.0	120.2	119.0	116.9	114.6	120.9	120.9	118.5
9	110.7	117.3	116.2	113.4	111.3	118.0	118.2	115.2
sum(7−9)	338.8	357.9	354.4	347.0	340.6	360.0	360.1	352.1
10	118.3	118.8	119.1	118.8	116.7	117.4	118.2	117.8
11	118.5	116.5	117.3	117.4	120.9	116.8	118.0	118.6
12	123.2	125.0	124.0	123.4	121.7	125.0	123.4	122.5
13	116.3	116.0	116.5	116.9	116.2	115.9	116.9	117.1
14	121.6	120.9	121.3	122.0	122.3	120.5	121.1	122.1
15	122.0	122.7	121.8	121.6	122.1	124.5	122.5	122.0

us to choose various configuration spaces. Therefore, examination of the effect of the configuration space on the vertical excitation energy is essential. We first examined the dependence

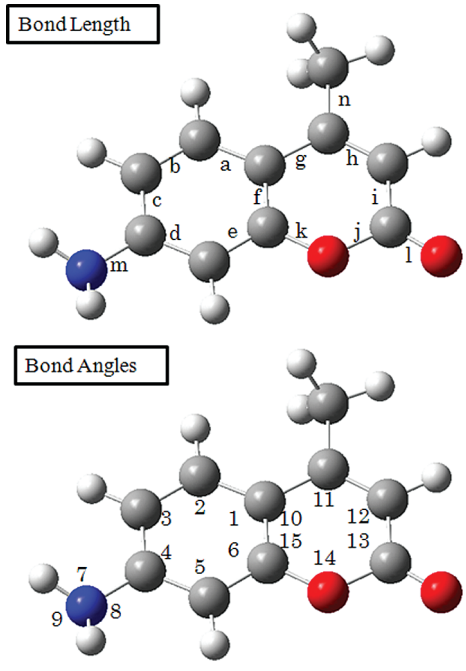

Figure 2. Designation of bonds and bond angles of C120 and C151.

TABLE 2: General Configuration Space Dependence of the GMC-QDPT and Active Space Dependence of MC-QDPT Excitation Energies (eV) of the First Excited State of C120 and C151

electron/orbital	no. of CSFs or SDs	coumarin120	coumarin151
GCS(6,6)	282 SDs	4.19	3.80
GCS(8,8)	1281 SDs	3.58	3.47
GCS(10,10)	7565 SDs	4.04	3.55
GCS(12,12)	21196 SDs	4.14	3.55
GCS(14,14)	48055 SDs	3.72	3.50
GCS(16,16)	94586 SDs	3.81	3.44
GCS(20,15)	54790 SDs	3.99	3.26
GCS(20,16)	90932 SDs	3.66	3.47
GCS(20,17)	137054 SDs	3.66	
CAS(6,6)	175 CSFs	2.99	3.36
CAS(8,8)	1764 CSFs	3.14	3.84
CAS(10,10)	19404 CSFs	3.91	4.16
CAS(12,12)	382239 CSFs		
CAS(14,14)	5010005 CSFs		
experiment[a]		3.51	3.25

[a] Reference 30.

of the excitation energies obtained by GMC-QDPT on the general configuration space and reference wave function. Table 2 lists the dependence of the excitation energies of the first excited state of C120 and C151 on the general configuration space. The number of configurations considered in the GCS or CAS is also listed in Table 2. The number of configurations in GCS is the number of Slater determinants (SD), while the number of configurations in CAS is the number of configuration

state functions (CSF). Starting from GCS(6,6), where GCS(n,m) means the general configuration space constructed from n electrons and m orbitals, as the configuration space size increases, the excitation energy slowly converges toward the experimental value.[30] For comparison, we have also calculated MC-QDPT utilizing CASSCF reference functions with active space starting from CAS(6,6), where CAS(n,m) means the complete active space constructed from n electrons and m orbitals. The experimental values were recorded in ethanol and the spectra showed strong red shifts, and thus the excitation energies in the gas phase are expected to be slightly higher than the experimental data. Both C120 and C151 results from GMC-QDPT converge to values above the experimental values, as expected.

For C120, 20 electrons and 17 orbitals were necessary to include all valence π, π^*, and n orbitals in the GCS. For the guess orbitals for our GMC-QDPT calculation, we utilized the RHF orbitals. The LUMO, LUMO+1, and LUMO+2 of RHF calculations has pure π character. On the other hand, mixture of the characters in the orbitals with higher energy was found. Figure S2 and S3 in the Supporting Information lists the RHF orbitals and the GMC-SCF natural orbitals, respectively. As shown in Figure S2, the RHF virtual orbitals have mixed characters. On the other hand, GMC-SCF natural orbitals in Figure S3 have pure π character. Thus, we needed seventeen orbitals for our calculation.

For C151, 20 electrons and 16 orbitals were necessary to include all valence π, π^*, and n orbitals in the GCS. On the other hand, CASSCF referenced MC-QDPT does not converge because of the small active space and has large errors. MC-QDPT calculations were not possible with CAS(20,17) or CAS(20,16) because of the enormous number of configuration state functions (CSFs). The MC-QDPT results show the importance of using a large active space to include all valence π and n orbitals and electrons for the MC reference perturbation calculations. Because the excitation energies seem to be converging, we used the data obtained from GCS(20,17) for C120, and GCS(20,16) for C151 for further discussion of the absorption spectra.

In our preliminary calculations, we have also surveyed the convergence of the absorption spectra to the reference space, i.e., the number of parent configurations in our GMC calculation. We calculated the absorption spectra using different numbers of parent configurations to seek the convergence. We found that the difference between absorption spectra calculated using 35 and 45 parent configurations was less than 0.04 eV among the tested GCSs. Thus, we decided to use 45 parent configurations in our calculations.

In this article, GMC-QDPT absorption spectra are calculated using MP2 optimized structure. We have compared GMC-QDPT calculated absorption spectra using MP2 optimized structures and B3LYP optimized structures. The excitation energy of the lowest excited state differs by only 0.02 eV. Thus, we discuss the absorption spectra using MP2 optimized structure later on.

To study the low-lying excited states of C120 and C151 in detail, we chose the first six states for both molecules. Table 3 shows the main configurations with absolute values of coefficients over 0.1 of the excited states of C120 and C151. Tables 4 and 5 list the excitation energies and oscillator strengths of C120 and C151, respectively. The occupied orbitals of C120 and C151 are designated by 1, 2, 3, ..., from the highest orbital down, and the unoccupied orbitals by 1′, 2′, 3′, ..., from the lowest orbital up.

TABLE 3: Main Configurations of the Low-lying Singlet Excited States of C120 and C151

	C120		C151	
state	transitions	weight	transitions	weight
1^1A	HF configuration	0.894	HF configuration	0.888
2^1A	1 → 1′	0.558	1 → 1′	0.456
3^1A	1 → 2′	0.246	2 → 1′	0.233
	2 → 1′	0.205	1 → 2′	0.182
			1 → 1′	0.171
4^1A	2 → 1′	0.228	2 → 1′	0.162
	1 → 3′	0.133	1 → 3′	0.132
			1 → 2′	0.118
5^1A	4 → 1′	0.620	4 → 1′	0.630
	4 → 3′	0.125	4 → 3′	0.124
6^1A	3 → 1′	0.224	3 → 1′	0.140
	$(1)^2 \rightarrow (1')^2$	0.186	$(1)^2 \rightarrow (1')^2$	0.139
			2 → 1′	0.117
7^1A	1 → 3′	0.132	1 → 3′	0.184
	1 → 2′	0.131	3 → 1′	0.181
	2 → 1′	0.117	2 → 2′	0.111
	2 → 2′	0.109		
	3 → 1′	0.105		

TABLE 4: Calculated Excitation Energies (eV) of C120[a]

state	GMC-SCF	GMC-QDPT MP2opt	GMC-QDPT B3LYP opt	TDDFT B3LYP	experiment
2^1A	5.74	3.66 (0.2452)	3.64 (0.3000)	4.03 (0.3234)	3.51[b]
3^1A	6.95	4.14 (0.1585)	4.12 (0.1335)	4.48 (0.001)	
4^1A	4.86	4.52 (0.0510)	4.51 (0.0511)	5.02 (0.0393)	
5^1A	5.21	4.74 (0.0011)	4.80 (0.0012)	4.54 (0.0001)	
6^1A	6.42	5.26 (0.0068)	5.26 (0.0121)	5.51 (0.0013)	
7^1A	7.78	5.45 (0.3541)	5.49 (0.3562)	5.96 (0.1398)	5.35[b]

[a] The oscillator strengths are given in the parentheses. [b] Reference 30.

TABLE 5: Calculated Excitation Energies (eV) of C151[a]

state	GMC-SCF	GMC-QDPT	TDDFT B3LYP	experiment
2^1A	5.36	3.47 (0.3217)	3.77 (0.3093)	3.25[b]
3^1A	4.76	3.89 (0.0759)	4.22 (0.0029)	
4^1A	6.65	4.30 (0.0198)	4.95 (0.0265)	
5^1A	4.88	4.50 (0.0012)	4.33 (0.0001)	
6^1A	6.20	5.12 (0.0330)	5.43 (0.0346)	
7^1A	7.52	5.26 (0.1505)	5.81 (0.0867)	

[a] The oscillator strengths are given in parentheses. [b] Reference 30.

The ground state was well described by the Hartree−Fock configuration. The first excited state of C120 and C151 results from the 1 (HOMO) → 1′ (LUMO) transition, where orbital 1 is a π orbital and 1′ is a π^* orbital. This state has a large oscillator strength, and thus we have assigned this state to the first peak in the experimental spectrum.[30] TDDFT results are larger than the experimental value by nearly 0.50 eV. The excitation energies of the first singlet excited state obtained by GMC-QDPT for both C120 and C151 are slightly above the experimental value recorded in ethanol.[30] In a previous work of ours,[29] we calculated the red shift of the excitation energy of C120 to be 0.32 eV using the polarizable continuum model.[54−56] Thus, TDDFT results become slightly above the experimental value and GMC-QDPT calculation becomes slightly below the experimental value. Both methods agree with the experimental data. The difference in the excitation energies between C120 and C151 results from the effect of substitution of the methyl group by the trifluoromethyl group. The substitution leads to a 0.19 eV decrease in the GMC-QDPT calculations. This agrees with the experimental value of 0.26 eV.[30]

TABLE 6: General Configuration Space Dependence of the Calculated Fluorescence Spectra (eV) of C120 and C151 with CIS Optimized Geometry

electron/orbital	no. of SDs	C120	C151
6/6	282 SDs	4.10	3.60
8/8	1281 SDs	3.28	3.57
10/10	7565 SDs	3.19	2.90
20/15	54790 SDs	3.23	3.11
20/16	90932 SDs	3.30	3.14
20/17	137054 SDs	3.24	
experiment[a]		2.91	2.58

[a] Reference 30.

The next two excited states of C151 are both described by 1 → 2′ (next LUMO) and 2 (next HOMO) → 1′ transitions, where 2 is a π orbital and 2′ is a π^* orbital. The oscillator strength of the second state is larger than that of the third state in our GMC-QDPT calculation. TDDFT results do not agree with the GMC-QDPT results for these two states. For the 3^1A state, the 1 → 1′ transition has a large contribution especially for C151. This leads to large oscillator strengths in this state for C120 and C151, as seen in the first excited state. The coefficients for 1 → 2′ are smaller than for 2 → 1′, and 3 → 1′ has a larger contribution in 4^1A, where 3 is a π orbital. We assigned the second excited state of C120 to the shoulder of the observed spectra in ethanol found at around 33 000 cm^{-1}.[30] The GMC-QDPT excitation energy is 4.14 eV, which agrees very well with experiment.

The fourth excited state of C120 and C151 has a different character compared with the other excited states. This excited state is described as arising from the 4 → 1′ and 4 → 3′ transitions, where 4 is the orbital of the lone pair electrons of the oxygen atom of C═O. This $n \rightarrow \pi^*$ excited state is found lower in energy than the third excited state in TDDFT.

The largest configurations of the fifth and sixth excited states for C120 and C151 are 3 → 1′ and 1 → 3′ transitions, respectively, where 3 is a π orbital and 3′ is a π^* orbital. Unlike the second and third excited states, the latter has a larger oscillator strength. The fifth excited state has contributions of 3 → 1′ and $(1)^2 \rightarrow (1')^2$ transitions for C120, and 3 → 1′, $(1)^2 \rightarrow (1')^2$, and 2 → 1′ transitions for C151. The main configurations of the sixth excited states are 1 → 3′, 1 → 2′, 2 → 1′, 2 → 2′, and 3 → 1′ and 3 → 1′, 1 → 3′, and 2 → 2′, for C120 and C151, respectively. We have assigned the sixth state with the large oscillator strength of C120 to the second peak of the observed absorption spectrum found in the range 43 000−44 000 cm^{-1}.[30] GMC-QDPT calculated the excitation energy of this state as 5.45 eV, which agrees very well with the experimental data. In our GMC-QDPT calculations, we expect the second peak of the absorption spectra to show a red shift of about 0.19 eV by substitution of the methyl group at the 4-position by the trifluoromethyl group.

C. Fluorescence Spectra. The GMC-QDPT method was used to calculate the fluorescence spectra from the structures optimized at the excited state. CIS and TDDFT with B3LYP and CAM-B3LYP functionals were used for optimization. We first examined the general configuration space dependence of the excitation energies with the CIS optimized structures. Table 6 lists the dependence of the calculated fluorescence energies of C120 and C151 on the general configuration space. As in the absorption spectra calculations, as the configuration space size increases, the excitation energy slowly converges toward the experimental value. For C120, 20 electrons and 17 orbitals were necessary to include all valence π, π^*, and n orbitals in the GCS. For C151, 20 electrons and 16 orbitals were necessary to include all valence π, π^*, and n orbitals in the GCS. These orbitals were the same as the orbitals used to calculate the vertical excitation energies. Because the fluorescence energies seem to be converging, we used the data obtained from GCS(20,17) for C120 and GCS(20,16) for C151 for further discussion.

TABLE 7: Calculated Fluorescence Energies of C120 and C151

	TDDFT		GMC-QDPT	experiment
C120 (CIS opt)	B3LYP	3.80	3.24	2.91[a]
C120 (B3LYP opt)	B3LYP	3.69	3.22	
C120 (CAM-B3LYP opt)	CAM-B3LYP	3.90	3.24	
C151 (CIS opt)	B3LYP	3.59	3.14	2.58[a]
C151 (B3LYP opt)	B3LYP	3.26	2.97	
C151 (CAM-B3LYP opt)	CAM-B3LYP	3.67	3.03	

[a] Reference 30.

Table 7 shows the calculated fluorescence energies. For the CIS optimized structures, the fluorescence energy of C120 computed by TDDFT B3LYP was 3.80 eV. This value overestimates the experimental value by more than 0.70 eV. The C120 fluorescence energy computed by GMC-QDPT was 3.24 eV. The GMC-QDPT calculation shows better agreement with the experimental data[30] compared with the result obtained by the TDDFT calculation with the B3LYP functional. For the TDDFT B3LYP optimized structure, the fluorescence energy computed by TDDFT B3LYP was 3.69 eV, while GMC-QDPT calculation shows better performance than the B3LYP calculation and predicted 3.22 eV. For the TDDFT CAM-B3LYP optimized structure, the fluorescence energy calculated by TDDFT CAM-B3LYP was 3.90 eV, which overestimated the observed data by nearly 1.0 eV. The fluorescence energy calculated by GMC-QDPT was 3.24 eV. In spite of the structure difference between the three different methods for optimization of the first excited state, GMC-QDPT predicted similar fluorescence energies. The experimental value was recorded in ethanol,[30] and thus consideration of the solvent effect in the GMC-QDPT calculation will lead to a large red shift of the fluorescence energies and better agreement with the experimental data.

The fluorescence energies calculated by TDDFT B3LYP of C151 was 3.59 eV for the CIS optimized structure, while GMC-QDPT calculation predicted 3.14 eV. For the TDDFT B3LYP structures, the fluorescence energy calculated by TDDFT B3LYP and GMC-QDPT was 3.26 and 2.97 eV, respectively. For the TDDFT CAM-B3LYP optimized structure, the fluorescence energy calculated by TDDFT CAM-B3LYP and GMC-QDPT was 3.67 and 3.03 eV, respectively. GMC-QDPT improves the TDDFT calculated fluorescence energies, which greatly overestimate the experimental value. Inclusion of the solvent effect in our GMC-QDPT calculation will lead to good agreement with the experimental data. We conclude that the calculated fluorescence spectra using the optimized geometry for the first excited state with a planar amino group with a CN single bond agrees well with the observed fluorescence spectra. Our results are consistent with the experimental data in nonpolar solvents.[17,18]

Conclusions

We have studied the low-lying excited states of C120 and C151 by employing GMC-QDPT and TDDFT. For the absorption spectra, both methods were in good agreements with the experimental data. On the other hand, GMC-QDPT showed

better agreements with the experimental data for the fluorescence spectra compared to TDDFT calculations.

MC-QDPT calculations utilizing CASSCF reference functions were also performed. The limiting size of the active space for the reference function leads to large errors. The GMC-QDPT calculation with all valence π and n electrons and orbitals converged to the experimental data. This shows the importance of including all valence π and n electrons and orbitals in calculations employing general MC reference perturbation theory.

We have elucidated the electronic structures of the low-lying excited states of C120 and C151 and explained the shape of the observed absorption spectra.

We found agreement between the observed fluorescence spectra and the GMC-QDPT results using optimized structures at the first excited state with a planar amino group.

In this study, we computed the excitation energies in the gas phase. In our forthcoming work, the solvent effect will be included. In previous studies, the importance of the hydrogen bond has been emphasized.[20] Thus, the solvent effect must be included explicitly. The QM/MM method[57] is a good candidate to model the 7-aminocoumarins in a solvent. Using QM/MM, we can combine molecular dynamics to obtain stochastic properties and study the dynamics in the solvent.

Acknowledgment. Y.K. was supported by the Program for Improvement of the Research Environment for Young Researchers from the Special Coordination Funds for Promoting Science and Technology (SCF), Japan. H.N. is grateful to CREST, Japan Science and Technology Agency (JST) for funding this research.

Supporting Information Available: Table of geometrical parameters. Figures of HOMOS and LUMOs. This material is available free of charge via the Internet at http://pubs.acs.org.

References and Notes

(1) Hirao, K. *Chem. Phys. Lett.* **1992**, *190*, 374–380.
(2) Hirao, K. *Chem. Phys. Lett.* **1992**, *196*, 397–403.
(3) Hirao, K. *Int. J. Quantum Chem.* **1992**, *S26*, 517–526.
(4) Nakano, H. *J. Chem. Phys.* **1993**, *99*, 7983–7992.
(5) Nakano, H. *Chem. Phys. Lett.* **1993**, *207*, 372–378.
(6) Hirao, K.; Nakano, H.; Hashimoto, T. *Chem. Phys. Lett.* **1995**, *235*, 430–435.
(7) Tsuneda, T.; Nakano, H.; Hirao, K. *J. Chem. Phys.* **1995**, *103*, 6520–6528.
(8) Nakano, H.; Tsuneda, T.; Hashimoto, T.; Hirao, K. *J. Chem. Phys.* **1996**, *104*, 2312–2320.
(9) Hashimoto, T.; Nakano, H.; Hirao, K. *J. Chem. Phys.* **1996**, *104*, 6244–6258.
(10) Kawashima, Y.; Nakayama, K.; Nakano, H.; Hirao, K. *Chem. Phys. Lett.* **1997**, *267*, 82–90.
(11) Nakayama, K.; Nakano, H.; Hirao, K. *Int. J. Quantum Chem.* **1998**, *66*, 157–175.
(12) Hashimoto, T.; Nakano, H.; Hirao, K. *J. Mol. Struct. (THEOCHEM)* **1998**, *451*, 25–33.
(13) Kawashima, Y.; Hashimoto, T.; Nakano, N.; Hirao, K. *Theor. Chem. Acc.* **1999**, *102*, 49–64.
(14) Nakano, H.; Uchiyama, R.; Hirao, K. *J. Comput. Chem.* **2002**, *23*, 1166–1175.
(15) Miyajima, M.; Watanabe, Y.; Nakano, H. *J. Chem. Phys.* **2006**, *124*, 044101.
(16) Ebisuzaki, R.; Watanabe, Y.; Nakano, H. *Chem. Phys. Lett.* **2007**, *442*, 164–169.
(17) Pal, H.; Nad, S.; Kumbhakar, M. *J. Chem. Phys.* **2003**, *119*, 443–452.
(18) Nad, S.; Pal, H. *J. Phys. Chem. A* **2001**, *105*, 1097–1106.
(19) Jones, G. II.; Jackson, W. R.; Choi, C.-Y.; Bergmark, W. R. *J. Phys. Chem.* **1985**, *89*, 294–300.
(20) Arbeloa, T. L.; Arbeloa, F. L.; Tapia, M. J.; Arbeloa, I. L. *J. Phys. Chem.* **1993**, *97*, 4704–4707.
(21) McCarthy, P. K.; Blanchard, G. J. *J. Phys. Chem.* **1993**, *97*, 12205–12209.
(22) Ando, K. *J. Chem. Phys.* **1997**, *107*, 4585–4596.
(23) Neugebauer, J.; Jacob, C. R.; Wesolowski, T. A.; Baerends, E. J. *J. Phys. Chem. A* **2005**, *109*, 7805–7814.
(24) Sulpizi, M.; Röhrig, U. F.; Hutter, J.; Rothlisberger, U. *Int. J. Quantum Chem.* **2004**, *101*, 671–682.
(25) Sulpizi, M.; Carloni, P.; Hutter, J.; Rothlisberger, U. *Phys. Chem. Chem. Phys.* **2003**, *5*, 4798–4805.
(26) Nguyen, K. A.; Day, P. N.; Pachter, R. *J. Chem. Phys.* **2007**, *126*, 094303.
(27) Cave, R. J.; Burke, K.; Castner, E. W., Jr. *J. Phys. Chem. A* **2002**, *106*, 9294–9305.
(28) Kina, D.; Arora, P.; Nakayama, A.; Noro, T.; Gordon, M. S.; Taketsugu, T. *Int. J. Quantum Chem.* **2009**, *109*, 2308–2318 (Prof. Hirao issue).
(29) Sakata, T.; Kawashima, Y.; Nakano, H. *Int. J. Quantum Chem.* **2009**, *109*, 1940–1949 (Prof. Hirao issue).
(30) Kitamura, N.; Fukagawa, T.; Kohtani, S.; Kitoh, S.; Kunimoto, K.; Nakagaki, R. *J. Photochem. Photobiol. A Chem.* **2007**, *188*, 378–386.
(31) Nakagaki, R.; Kitamura, N.; Aoyama, I.; Ohtsubo, H. *J. Photochem. Photobiol. A Chem.* **1994**, *90*, 113–119.
(32) Arbeloa, T. L.; Arbeloa, F. L.; Arbeloa, I. L. *J. Lumin.* **1996**, *68*, 149–155.
(33) Gustavsson, T.; Cassara, T. L.; Gulbinas, V.; Gurzadyan, G.; Mialocq, J.-C.; Pommeret, S.; Sorgius, M.; van der Meulen, P. *J. Phys. Chem. A* **1998**, *102*, 4229–4245.
(34) Chen, Y.; Palmer, P. M.; Topp, M. R. *Int. J. Mass Spectrom.* **2002**, *220*, 231–251. Sharma, V. K.; Saharo, P. D.; Sharma, N.; Rastogi, R. C.; Ghoshal, S. K.; Mohan, D. *Spectrochim. Acta Part A* **2003**, *59*, 1161–1170.
(35) Das, K.; Jain, B.; Patel, H. S. *J. Phys. Chem. A* **2006**, *110*, 1698–1704.
(36) Moog, R. S.; Kim, D. D.; Oberle, J. J.; Ostrowski, S. G. *J. Phys. Chem. A* **2004**, *108*, 9294–9301.
(37) Mühlpfordt, A.; Schanz, R.; Ernsting, N. P.; Farztdinov, V.; Grimme, S. *Phys. Chem. Chem. Phys.* **1999**, *1*, 3209–3218.
(38) Kurashige, Y.; Nakajima, T.; Kurashige, S.; Hirao, K.; Nishikitani, Y. *J. Phys. Chem. A* **2007**, *111*, 5544–5548.
(39) Improta, R.; Barone, V.; Santoro, F. *Angew. Chem.* **2007**, *119*, 409–412.
(40) Runge, E.; Gross, E. K. U. *Phys. Rev. Lett.* **1984**, *52*, 997–1000.
(41) Casida, M. *In Recent Advances in Density Functional Methods*; Chong, D. P. , Ed.; World Scientific: Singapore, 1995; Vol. 1, pp 155−192.
(42) Bauernschmitt, R.; Ahlrichs, R. *Chem. Phys. Lett.* **1996**, *256*, 454–464.
(43) Stratmann, R. E.; Scuseria, G. E.; Frisch, M. J. *J. Chem. Phys.* **1998**, *109*, 8218–8224.
(44) Furche, F.; Ahlrichs, R. *J. Chem. Phys.* **2002**, *117*, 7433–7477.
(45) Furche, F.; Ahlrichs, R. *J. Chem. Phys.* **2004**, *121*, 12772–12773.
(46) Becke, A. D. *J. Chem. Phys.* **1993**, *98*, 5648–5652.
(47) Becke, A. D. *Phys. Rev. A* **1988**, *38*, 3098–3100.
(48) Lee, C.; Yang, W.; Parr, R. G. *Phys. Rev. B* **1988**, *37*, 785–789.
(49) Yanai, T.; Tew, D. P.; Handy, N. C. *Chem. Phys. Lett.* **2004**, *393*, 51–57.
(50) Dunning, T. H. *J. Chem. Phys.* **1989**, *90*, 1007–1023.
(51) Frisch, M. J.; Trucks, G. W.; Schlegel, H. B.; Scuseria, G. E.; Robb, M. A.; Cheeseman, J. R.; Montgomery, J. A., Jr.; Vreven, T.; Kudin, K. N.; Burant, J. C.; Millam, J. M.; Iyengar, S. S.; Tomasi, J. J.; Barone, V.; Mennucci, B.; Cossi, M.; Scalmani, G.; Rega, N.; Petersson, G. A.; Nakatsuji, H.; Hada, M.; Ehara, M.; Toyota, K.; Fukuda, R.; Hasegawa, J.; Ishida, M.; Nakajima, T.; Honda, Y.; Kitao, O.; Nakai, H.; Klene, M.; Li, X.; Knox, J. E.; Hratchian, H. P.; Cross, J. B.; Adamo, C.; Jaramillo, J.; Gomperts, R.; Stratmann, R. E.; Yazyev, O.; Austin, A. J.; Cammi, R.; Pomelli, C.; Ochterski, J. W.; Ayala, P. Y.; Morokuma, K.; Voth, A.; Salvador, P.; Dannenberg, J. J.; Zakrzewski, V. G.; Dapprich, S.; Daniels, A. D.; Strain, M. C.; Farkas, O.; Malick, D. K.; Rabuck, A. D.; Raghavachari, K.; Foresman, J. B.; Ortiz, J. V.; Cui, Q.; Baboul, A. G.; Clifford, S.; Cioslowski, J.; Stefanov, B. B.; Liu, G.; Liashenko, A.; Piskorz, P.; Komaromi, I.; Martin, R. L.; Fox, D. J.; Keith, T.; Al-Laham, M. A.; Peng, C. Y.; Nanayakkara, A.; Challacombe, M.; Gill, P. M. W.; Johnson, B.; Chen, W.; Wong, M. W.; Gonzalez, C.; Pople, J. A. *Gaussian 09*, revision A.01; Gaussian, Inc.: Wallingford, CT, U.S., 2009.
(52) Schmidt, M. W.; Baldridge, K. K.; Boatz, J. A.; Elbert, S. T.; Gordon, M. S.; Jensen, J. H.; Koseki, S.; Matsunaga, N.; Nguyen, K. A.; Su, S.; Windus, T. L. *J. Comput. Chem.* **1993**, *14*, 1347–1363.
(53) Kobayashi, R.; Amos, R. D. *Chem. Phys. Lett.* **2006**, *420*, 106–109.
(54) Tomasi, J.; Mennucci, B.; Cammi, R. *Chem. Rev.* **2005**, *105*, 2999–3093.
(55) Cossi, M.; Barone, V. *J. Chem. Phys.* **2001**, *115*, 4708–4717.
(56) Improta, R.; Barone, V.; Scalmani, G.; Frisch, M. *J. Chem. Phys.* **2006**, *125*, 54103.
(57) Warshel, A.; Levitt, M. J. *J. Mol. Biol.* **1976**, *103*, 227–249.

JP1019872